Simulation of the ultrasonic wave propagation in solids

R. Barauskas, V. Daniulaitis

Kaunas University of Technology

Mickevičiaus g. 37, 3004 Kaunas

Introduction

Historically, nondestructive testing (NDT) has been used for detecting macroscopic and microscopic discontinuities in structures after they have been in service for some time or in new ones. The prominent role in nondestructive testing ultrasonic has won because of the application versatility, sensitivity and convenience. It has become evident that it is practical and cost effective to expand the role of the testing to include all aspects of materials and structures production and application. The main research efforts are being directed at developing nondestructive techniques capable of monitoring production process, material integrity, the amount and rate of degradation during service. However, comprehensive understanding of the processes taking place in the testing specimen is available only by fully investigating testing instrumentation and method. It includes analysis of the characteristics of the equipment being used and analysis of the wave propagation in the structure under investigation. The task is rather complicated, because the series of the signal transformations from electrical to mechanical and vice versa are encountered, the behavior of the structure is predetermined in general by the non linear material properties and/or anisotropy. This problem could be treated as complex one, dealing with the problems of electrical and mechanical origin. This paper is devoted to the mechanical ones, trying to find ways for effective simulation of the signal propagation in the structure subjected to nondestructive testing. In many cases simplified methods (e.g., ray tracing) can be used, however they are not based upon the differential equations and, consequently, present only rough evaluation of the wave front propagation. On the other hand, finite element or finite difference methods enable to get adequate representation of the process, however, computer resource requirements are usually too great for problems of a practical value.

The situation can be improved by developing efficient algorithms of numerical modeling based on deeper analysis of the wave propagation phenomenon. Namely, large areas of the structure could be treated as homogenous rectangle zones with respect to the ultrasonic's signal wavelength and they could be meshed by uniform quadrilateral finite element mesh allowing to obtain the solution on a finite element level. Only boundary edges having complicated geometrical shape have to be approximated by comparatively small freely meshed zones

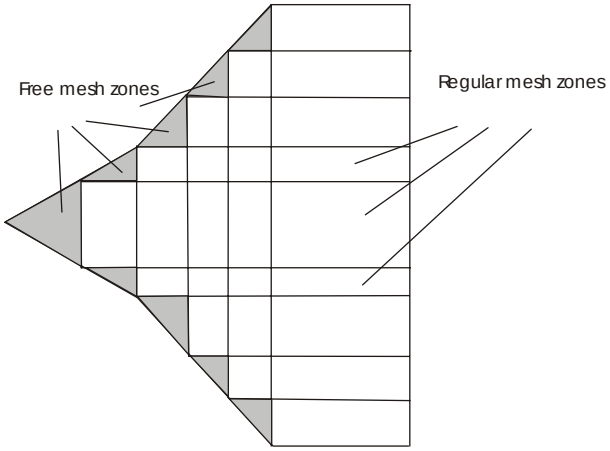

Fig.1. **Object's division scheme into rectangle and triangle zones**

(Fig.1).

Moreover, in the initial stages of the signal propagation there is comparatively small number of the nodes subjected to the excitation. Actually, model increases as the wave propagates (Fig. 2) and the possibility to control the model size could be of great interest and advantage.

In order to meet these specifications the finite element procedure in regular quadrilateral and free triangular finite

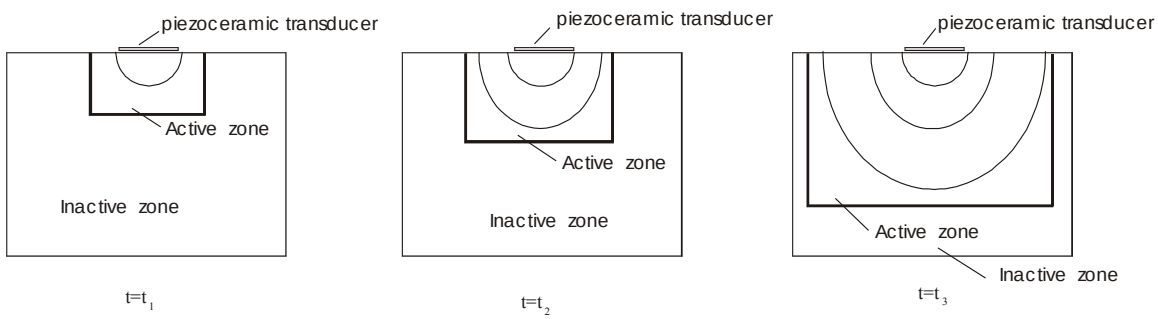

Fig.2. **Wave propagation in the object**

element meshes was developed and adopted for the short wave propagation modeling in NDT processes.

Application of the finite element method

A short wavelength elastic wave propagation analysis is performed by solving the structural dynamic equation

$$[M]\{\ddot{U}\}+[C]\{\dot{U}\}+[K]\{U\}=\{F(t)\}; \quad (1)$$

where $[M]$, $[K]$, $[C]=\alpha[M]$ - are the mass, stiffness and proportional damping matrices; $\{F\}$- the external load vector, $\{U\}$, $\{\dot{U}\}$, $\{\ddot{U}\}$ are the nodal displacement, velocity and acceleration vectors of the structure.

The time integration is being performed by means of the *central difference* integration scheme:

$$\{U_{t+\Delta t}\}=\left[\hat{M}\right]^{-1}\left[\{F_t\}-\left([K]-\frac{2}{\Delta t^2}[M]\right)\{U_t\}-\left[\tilde{M}\right]\{U_{t-\Delta t}\}\right] \quad (2)$$

where

$$\left[\hat{M}\right]=\frac{1}{\Delta t^2}[M]+\frac{1}{2\Delta t}[C]=\frac{1}{\Delta t^2}[M]+\frac{1}{2\Delta t}\alpha[M]; \quad (3)$$

$$\left[\tilde{M}\right]=\frac{1}{\Delta t^2}[M]-\frac{1}{2\Delta t}[C]=\frac{1}{\Delta t^2}[M]-\frac{1}{2\Delta t}\alpha[M], \quad (4)$$

were Δt is the time integration step.

Generally, the upper limit of discretization steps in space and time can be evaluated by means of the inequality

$$\frac{c\cdot\Delta t}{\Delta x}<1; \quad (5)$$

where c – is the velocity of the wave in the media, Δt, Δx are discretization steps in time and space respectively.

For elastic solid regions, containing several materials, we use the discretization steps based on the inequalities

$$\Delta x<\frac{C_{\min}}{5\omega_{ex}},\ \Delta t<\frac{\Delta X}{2c_{\max}} \quad (6)$$

where $c=\sqrt{\frac{E}{\rho}}$ is the velocity of propagation of the longitudinal wave , E – is the Young's modulus of the solid region and ρ is the density of the material. Values $c_{\min}, c_{\max}$ correspond to minimum and maximum values of the wave propagation velocity, if the structure contains several different materials. This leads to huge computational amounts even in 2D case. In steel regions with $c\approx 5200$ m/s and the excitation frequency $\omega_{ex}\geq 3$ MHz we obtain $\Delta x<5\times10^{-5}m$ and the necessary number of elements of the square plate of dimension $0.1m\times0.1m$ is about 4 million.

Concerning the NDT problems, the efficiency of the algorithms could be improved by taking in to account the specific features of the problem. As the approach should be oriented to very large models, the computational algorithm is being optimized as follows.

Large domains under investigation are subdivided into rectangular areas of uniform quadrilateral finite element meshes and small number of areas of arbitrary geometrical shape presented by free meshes (Fig. 1). The recursive formulae for obtaining nodal displacements could be derived by proper time integration scheme modification. For regular quadrilateral element meshes formulae (2) is used separately for every individual node. In this case $\left[\hat{M}\right]$and $\left[\tilde{M}\right]$ corresponds to a node's mass and only product $[K]\{U_t\}$ should be calculated.

The product $[K]\{U_t\}$ for the regular domains is being obtained on the element level and then assembled to nodal vector. As all the matrices of the elements in this domain are identical, the calculation of the product corresponding to node *ij* , see Fig. 3, can be presented by the recursive formula as

$$\begin{aligned}[K]\{U\}_{i,j}=&\left(\left[K^e_{11}\right]+\left[K^e_{22}\right]+\left[K^e_{33}\right]+\left[K^e_{44}\right]\right)\{U\}_{i,j}+\\&+\left(\left[K^e_{21}\right]+\left[K^e_{34}\right]\right)\{U\}_{i-1,j}+\left(\left[K^e_{23}\right]+\left[K^e_{14}\right]\right)\{U\}_{i,j+1}+\\&+\left(\left[K^e_{12}\right]+\left[K^e_{43}\right]\right)\{U\}_{i+1,j}+\left(\left[K^e_{41}\right]+\left[K^e_{32}\right]\right)\{U\}_{i,j-1}+\\&+\left[K^e_{24}\right]\{U\}_{i-1,j+1}+\left[K^e_{13}\right]\{U\}_{i+1,j+1}+\\&+\left[K^e_{42}\right]\{U\}_{i+1,j-1}+\left[K^e_{31}\right]\{U\}_{i-1,j-1}\end{aligned} \quad (7)$$

where $[K^e_{st}], s,t,=1,2,3,4$ are blocks of dimension 2x2 of the stiffness matrix of the quadrilateral element, the local nodal numbers of which are being assigned from the bottom left corner in counterclockwise direction.

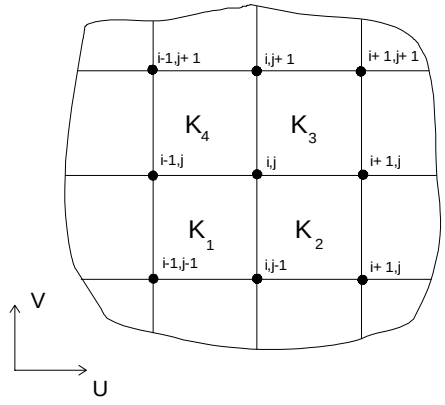

Fig. 3 **Fragment of the finite element model**

Formula (2) recalls the relations of the finite difference method described in [3], invoking similar number of arithmetic operations to be performed during each time integration step. However, the finite element approach avoids algorithmic difficulties encountered when the finite difference model has to be connected with adjacent regions of arbitrary shape modeled by free finite element meshes. The calculation of the displacements for freely meshed domains requires considerably greater amounts of computational time per node, however, usually the number

of nodes in such domains is small in comparison with the total number of nodes of the model.

Diagonal (lumped) mass and damping matrices are being used, therefore no matrix inverses are necessary in Eq. (2).

The domain regularly meshed by quadrilateral elements is subdivided into rectangular subdomains, displacements of which are stored as files on a hard disc. For each subdomain the activity index is supplied indicating if the wave has reached the subdomain. Inactive subdomains are excluded from computation of $[K]\{U_t\}$ and considerable time saving is achieved during first stages of the wave propagation. Similarly, the subdomains passed by the wave and containing only very small residual vibration are indicated as inactive and excluded from computation until they are reached by the next wavefront. It is necessary to mention, that the velocity of the excited wave propagation do not coincides with the rate at which the induced signal propagates in the finite element mesh. At the next time integration step non zero displacement value attains nodes, which surround the node that had started to vibrate at a previous time step, thus the signal propagating rate in the mesh is $\frac{\Delta x}{\Delta t}$. According to the inequality (5), it is at least 2 times greater than the actual velocity of the longitudinal wave. It is possible to reduce excitation rate by setting bigger time step, however that forces to utilize unconditionally stable algorithms. Dynamic stiffness matrices of these algorithms are not diagonal and inversion of it essentially reduces the efficiency of the method.

The technique proposed by means of filtering allows eliminate the numerical noise which propagates with a greater speed than the longitudinal wave. Displacements of the nodes are being set to zero value if they do not exceed a predefined threshold. Actually it is sufficient to nullify all the values below the $10^{-4} \times u_{\max}$, where $u_{\max}$ corresponds to the maximum value of the displacement since the start of program. Such checks of displacement values is being performed after every integration step.

Products $[K]\{U_t\}$ could be evaluated for every individual rectangular zone by using displacements of certain and adjacent zones. If matrices $[\hat{M}]$ and $[\tilde{M}]$ are diagonal, Eq. (2) is used for every zone separately. That allows to store in the random access memory only products $[K]\{U_t\}$ corresponding to the nodes shared by adjacent areas, while products $[K]\{U_t\}$ corresponding to the internal nodes of the area are stored on a hard disc.

Modeling strategies

The proposed algorithm has been developed for the investigation of the two dimensional model. Depending on the operating conditions, various plates or even three dimensional bodies like liquid/gas vessels, bearing rollers, fly-wheels could be examined by using two dimensional mathematical models.

For thin plate modeling the following steps should be performed. Firstly, geometrical model identical to the shape of the real object is formed. Model is subdivided into rectangular zones. Dimensions of the zones are defined in such a way that only whole (odd or even) number of finite elements of prescribed size could form boundaries of the zone. Inner and peripheral fully filled zones are meshed by a uniform quadrilateral finite element mesh. Since all finite elements are identical, only the stiffness matrix of a single element and nodal masses are necessary for performing computations. Zones, which are not rectangular, are considered as zones of a free shape and are meshed by a triangle mesh. For such zones the mass $[\hat{M}]$, $[\tilde{M}]$ and the stiffness $[K]$ matrices are formed and saved on a hard disc.

In the case of the axis symmetric problem the above

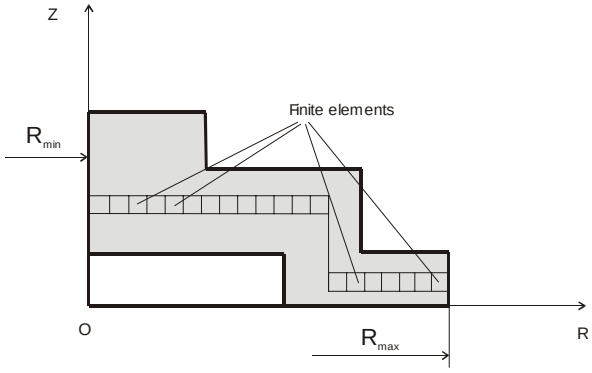

Fig. 4. **Axis symmetric specimen**

discussed algorithm is being modified by taking into account that finite element matrices of the elements are functions of their radial positions. Therefore the matrix of a thin radial strip is being assembled and used for making the matrix of the zone, see Fig 4.

Recursive formulae (7) for obtaining products $[K]\{U_t\}$ is being modified accordingly to Fig.5 as:

$$[K]\{U\}_{i,j} = [K^1_{31}]\{U\}_{i-1,j-1} + [K^1_{32}]\{U\}_{1,j-1} + [K^1_{33}]\{U\}_{i,j} +$$
$$+ [K^1_{34}]\{U\}_{i-1,j} + [K^4_{21}]\{U\}_{i-1,j} + [K^4_{22}]\{U\}_{i,j} + [K^4_{23}]\{U\}_{i,j+1} +$$
$$+ [K^4_{24}]\{U\}_{i-1,j+1} + [K^2_{41}]\{U\}_{i,j-1} + [K^2_{42}]\{U\}_{i+1,j-1} +$$
$$+ [K^2_{43}]\{U\}_{i+1,j} + [K^2_{44}]\{U\}_{i,j} + [K^3_{11}]\{U\}_{i,j} + [K^3_{12}]\{U\}_{i+1,j} +$$
$$+ [K^3_{13}]\{U\}_{i+1,j+1} + [K^3_{14}]\{U\}_{i,j+1} \qquad (8)$$

It is evident that the computation speed for axisymmetric models is lower in comparison with the plain stress or plain strain models because of additional case operators introduced by variety of finite element's matrices.

Another important factor to be discussed is the wave attenuation phenomenon. If attenuation factor is negligible,

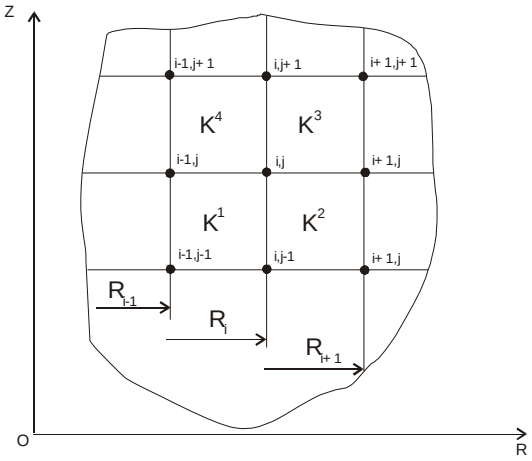

Fig. 5. **Fragment of axis symmetric model**

it could be excluded from the analysis without influencing the accuracy of the results. However, frequently it is necessary to take that fact into consideration. There is no algorithmic and program difficulties to model damped wave propagation. Recalling formulas (3) and (4) it can be observed that attenuation could be invoked by defining damping coefficient and disabled by setting that coefficient to zero. For regular zones that operation is performed during preprocessing step, and for freely mesh zones – during every integration step, causing a computational process to be a little longer, see Fig. 11.

Modeling results

Developed computer program was used to model a wave propagation process in plates and axisymmetric structures. Bellow we present some examples of the modeling results. Fig.6 and Fig.7 present two dimensional plain strain model with different damping ratio subjected to a single sinus-shaped excitation signal. The uniformly and freely meshed zones are clearly seen.

Fig.8 presents a displacement contour plot for the axisymmetric model subjected to an ultrasonic signal, see Fig.10. Below the same plain strain model is presented in

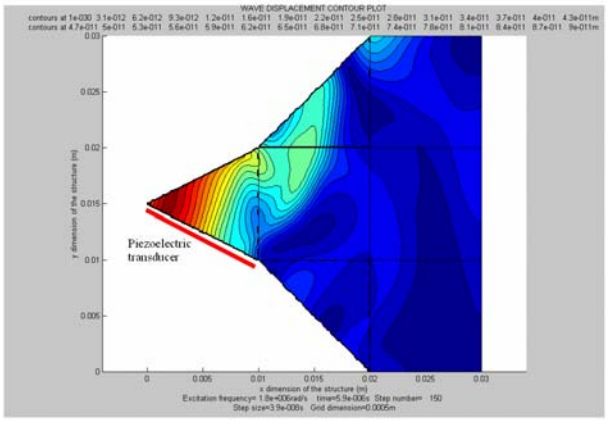

Fig. 6. **Displacement plot of undamped wave propagation; (signal frequency 1MHz, time=5.9 10^{-6} s).**

order to demonstrate differences between axisymmetric and plain strain models (Fig.9).

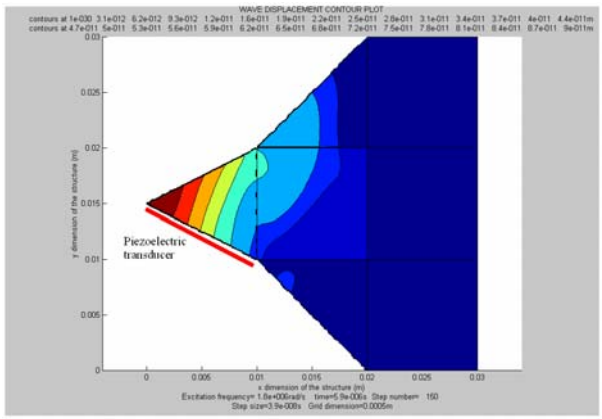

Fig. 7. **Displacement plot of damped wave propagation; (signal frequency 1MHz, time=5.9 10^{-6} s, damping ratio 10^6)**

Finally, summary of the computer time usage for damped and undamped planar and axisymmetric models is presented in Table 1 and Fig.11.

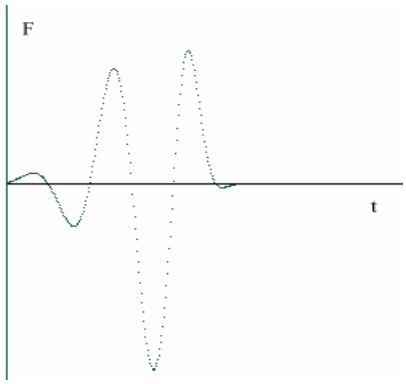

Fig.10. **Schematic of the excited signal**

Table 1

Model size (number of nodes)	Computer time used (min, sec)		
	Undamped model	Damped model	Axis symmetric model
10201	0,54	0,56	1,17

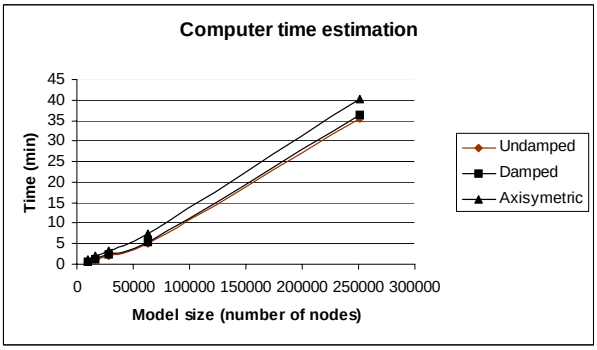

Fig.11. **Estimation of a computer time**

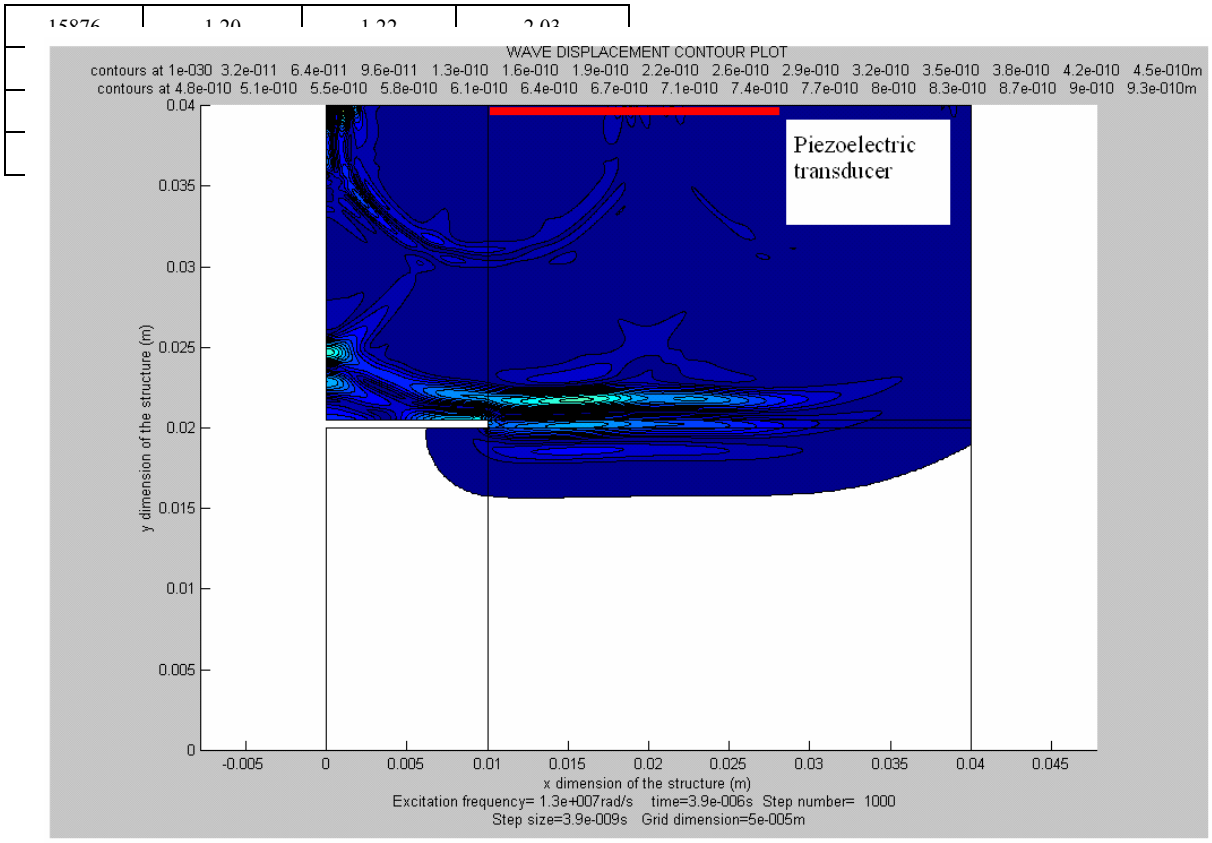

Fig. 8. **Displacement contour plot for wave propagation in axis symmetric model**

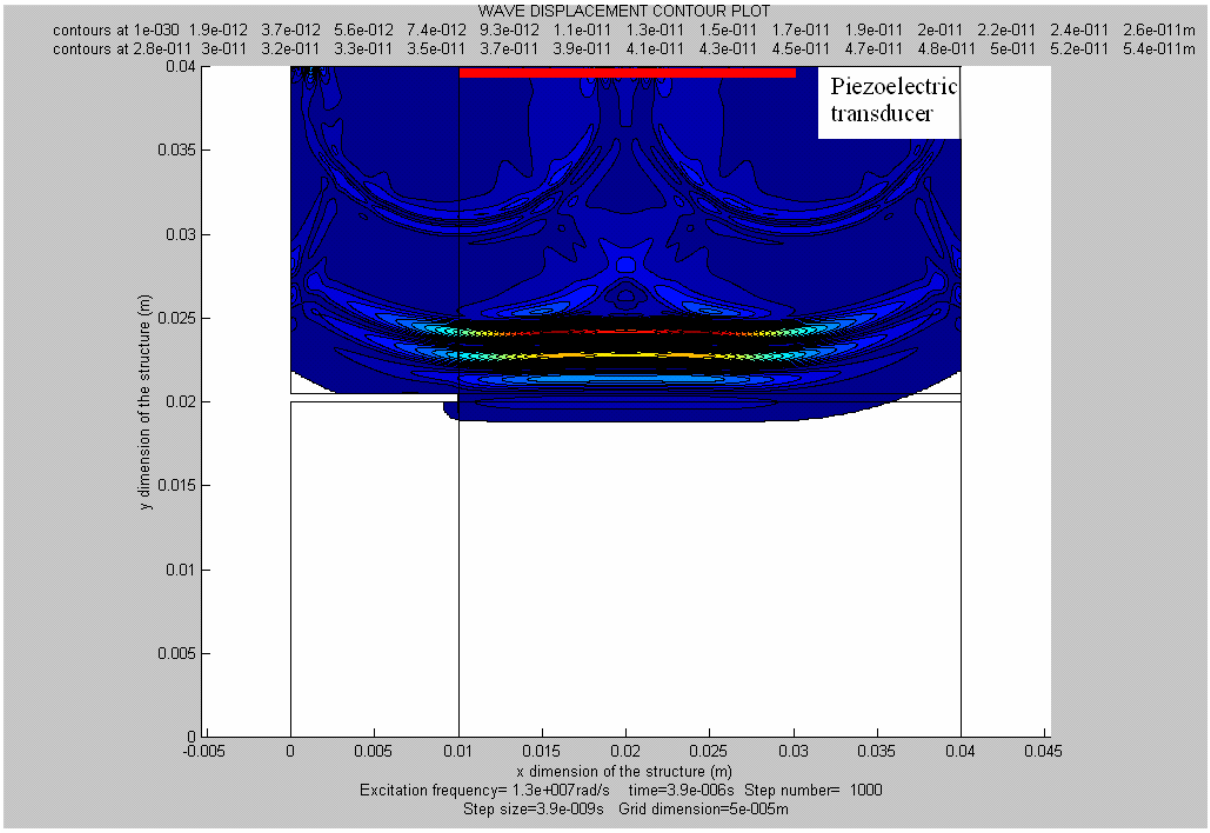

Fig.9. **Displacement contour plot for wave propagation in plain strain model**

Conclusions

Conventional methods, including finite element method, finite difference method or even combination of these methods do not provide solution of short wave propagation problems for cases of a practical value. All methods require refined model discretization and small a integration step size that inevitably leads to large models and huge amounts of computational resources. The improvement of the effectiveness of a numerical simulation can be achieved by using explicit time integration schemes in uniform finite element meshes. By comparing computational time for solution of the problem of dimension up to 200,000 nodes by the conventional finite element method and by the proposed technique, it was found that the latter technique is nearly 10 times faster. On the other hand, the proposed technique enables to create and analyze models, solution of which is practically impossible by most commercially available finite element codes, because of model size limitations.

References

1. **Argyris J.H., Doltsinis J.St., Knudson W.C., Vaz L.E., Willam K.J.** Numerical solution of transient nonlinear problems, Comp. Meths. Appl. Mech. Engng. 1979.17/18. P. 341-409.
2. **Bathe K.J., Wilson E.L**. Numerical methods in finite element analysis. - PRENTICE-HALL, INC., Englewood Cliffs, New Jersey;
3. **Harumi K**. Computer simulation of ultrasonics in a solid, NDT International. October 1986. Vol.19, N5. P.315-331.
4. **Komura I., Nakamura H.** Numerical Analysis of Elastic Wave Propagation in Simulation of Ultrasonic Examination, Proceedings of 7th Eropean Conference of Non-Destructive Testing. Copenhagen, 26-29 May 1998.
5. **Barauskas R.** On space and time step sizes in rectangular finite element meshes for ultrasonic pulse propagation, Ultragarsas, N1(34). 2000. P.47-53.

R Barauskas, V. Daniulaitis

Ultragarso bangų sklidimo kietame deformuojamame kūne modeliavimas

Reziumė

Išsamiai ištirti ultragarsinio matavimo proceso dinamiką galima tik skaitiškai sprendžiant diferencialines dalinių išvestinių lygtis baigtinių elementų arba baigtinių skirtumų metodais. Tačiau net ir nedideliems praktiniams uždaviniams išspręsti reikia didelių skaičiavimo resursų (laiko ir kompiuterio atminties), kadangi tradicinės baigtinių elementų arba baigtinių skirtumų metodų formuluotės neįvertina ultragarsinio matavimo proceso savitumų. Atsižvelgiant į tiriamo uždavinio specifiką, pasiūlytas ir programiškai sukurtas naujas baigtinių elementų metodo algoritmas dvimačiams modeliams tirti. Naudojant sukurtą programą, tirtos dvimatės ir ašiai simetrinės konstrukcijos. Gauti rezultatai leidžia teigti, kad uždavinys sprendžiamas vidutiniškai dešimt kartų sparčiau, palyginti su komerciniu baigtinių elementų programų paketu ANSYS, be to, programa iš principo leidžia nagrinėti didesnius modelius.

Pateikta spaudai 2000 12 11